



Associating Specific Somatic Mutations with Immune Infiltration Patterns in Metastatic Clear Cell Renal Cell Carcinoma



Nicholas H Chakiryan, Ali Hajiran, Youngchul Kim, Ahmet M Aydin, Logan Zemp, Esther Katende, Jonathan Nguyen, Wenyi Fan, Chia-Ho Cheng, Neale Lopez-Blanco, Jad Chahoud, Philippe E Spiess, Michelle Fournier, Jasreman Dhillon, Liang Wang, Carlos Moran-Segura, James Mulé, Dongliang Du, Anders Berglund, Jamie K Teer, and Brandon J Manley

H. LEE MOFFITT CANCER CENTER & RESEARCH INSTITUTE,
AN NCI COMPREHENSIVE CANCER CENTER – Tampa, FL
1-888-MOFFITT (1-888-663-3488) www.MOFFITT.org

© 2010 H. Lee Moffitt Cancer Center and Research Institute, Inc.

Background

Clear cell renal cell carcinoma (ccRCC) tumors have comparatively low frequencies of genetic alterations, yet very high levels of immune cell infiltration and favorable response rates to immunotherapy (IT) relative to other malignancies. Currently, the interplay between specific ccRCC somatic mutations and immune infiltration pattern is unclear. Identification of significant associations between common ccRCC somatic mutations and immune cell infiltration within the tumor immune microenvironment (TIME) could be impactful in both the research and clinical settings. Our primary objective is to analyze the associations between the most frequent somatic mutations in metastatic ccRCC and immune infiltration patterns within the TIME.

Methods

Tumor samples were obtained from patients with metastatic ccRCC. Targeted sequencing was used to identify the most frequent recurrent somatic mutations. Multiplex immunofluorescent (IF) tissue staining was used to assess TIME infiltration patterns within three distinct regions of interest (ROI): the tumor-core, adjacent stroma, and the tumor-stroma interface. Slides were sequentially stained in two panels, one for lymphoid and one for myeloid markers. Quantitative image analysis was utilized to generate counts for each cell by IF marker. For each tissue sample, cell density (cell count / total cell count) was determined for each IF marker and a subset of dual-positive markers. A linear mixed model analysis was performed to test associations between immune cell density for each IF marker at each of the three ROIs, and mutation status. Log-rank testing and multivariable Cox regression were used to analyze survival outcomes (Covariates: Age, gender, and IMDC risk score at diagnosis).

Variable	N = 48*
Median age at diagnosis, y	57 (39-77)
Median follow-up after diagnosis, mo	50 (12-178)
Median maximal tumor dimension, cm	10 (2.5-16.2)
Gender	
Male	33 (69%)
Female	15 (31%)
Race	
White	45 (94%)
Asian	1 (2%)
Black	0 (0%)
Other	2 (4%)
Fuhrman nuclear grade	
2	3 (6%)
3	29 (60%)
4	16 (34%)
Laterality	
Right	32 (66%)
Left	16 (34%)
pT†	
T1	4 (8%)
T2	8 (17%)
T3	29 (60%)
T4	7 (15%)
pN†	
N0	24 (50%)
N1	24 (50%)
pM†	
M0	18 (38%)
M1	30 (62%)
IMDC risk category‡	
Favorable-risk (0 criteria)	0 (0%)
Intermediate-risk (1-2 criteria)	23 (48%)
Poor-risk (≥ 3 criteria)	25 (52%)
Tissue specimen collection site	
Kidney	24 (50%)
Skin/soft tissue	10 (21%)
Bone	4 (8%)
Lung	3 (6%)
Retroperitoneum	2 (4%)
Brain	2 (4%)
Liver	1 (2%)
Colon	1 (2%)
Adrenal	1 (2%)
Lines of systemic therapy	3 (1 - 5)
Types of systemic therapy	
Immunotherapy	48 (100%)
Targeted therapy	32 (67%)
Immune checkpoint inhibition	19 (40%)
mTOR inhibitor	18 (38%)

* Results listed as Median (Range) or N (%)

† Pathologic staging is at the time of initial nephrectomy or metastasectomy. All patients in this study (n = 48) developed metastatic disease.

‡ IMDC (International Metastatic RCC Database Consortium) Risk Score is relevant to mRCC patients undergoing systemic therapy, and several ongoing trials are using this model in prospective studies. The criteria include: less than one year from time of diagnosis to systemic therapy, Karnofsky performance status < 80%, hemoglobin < lower limit of normal, calcium > upper limit of normal, neutrophil count > upper limit of normal, and platelet count > upper limit of normal.

Table 1. Baseline Patient and Specimen Demographics

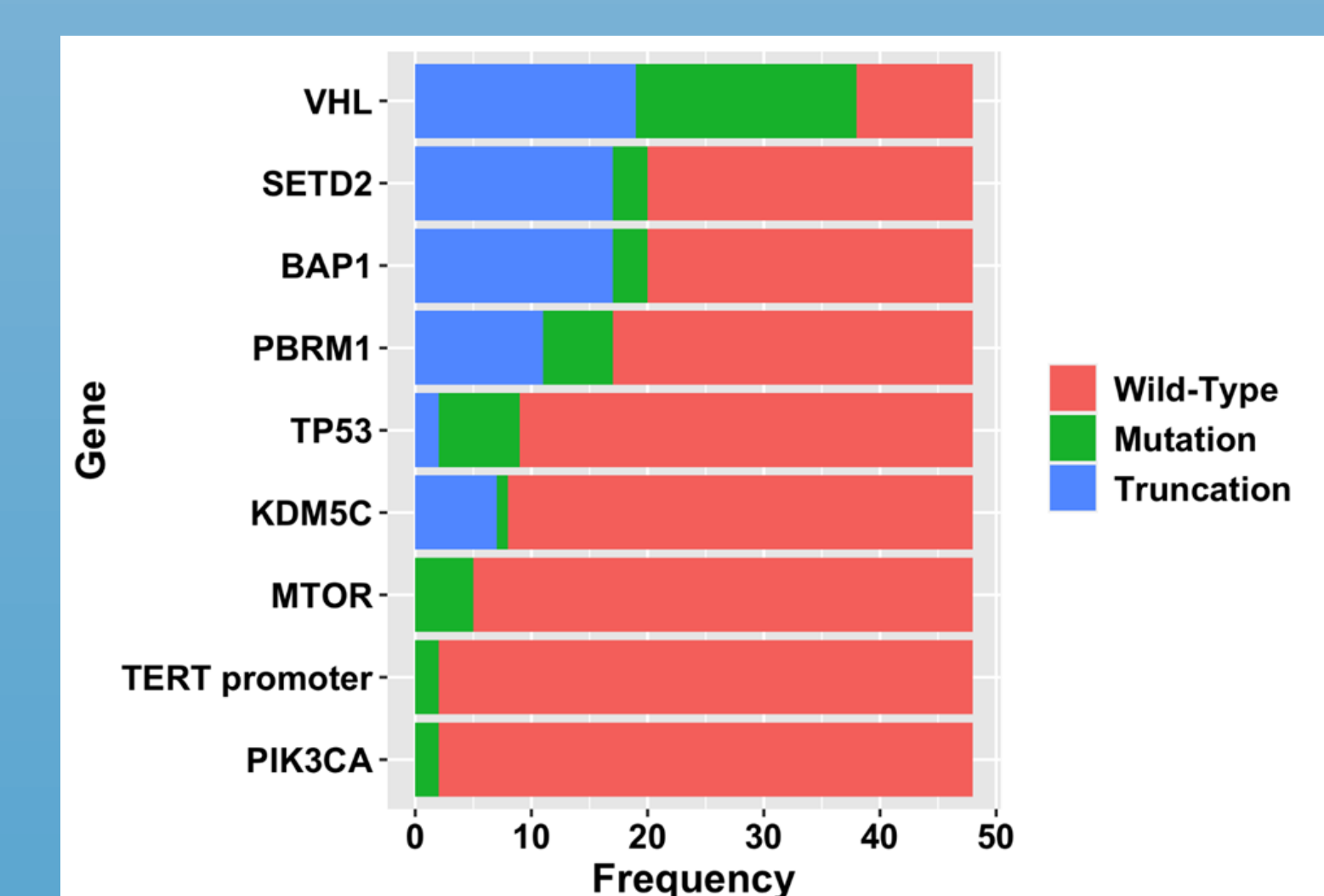


Figure 1. Bar-diagram of identified somatic mutations among the cohort of primary tumors.

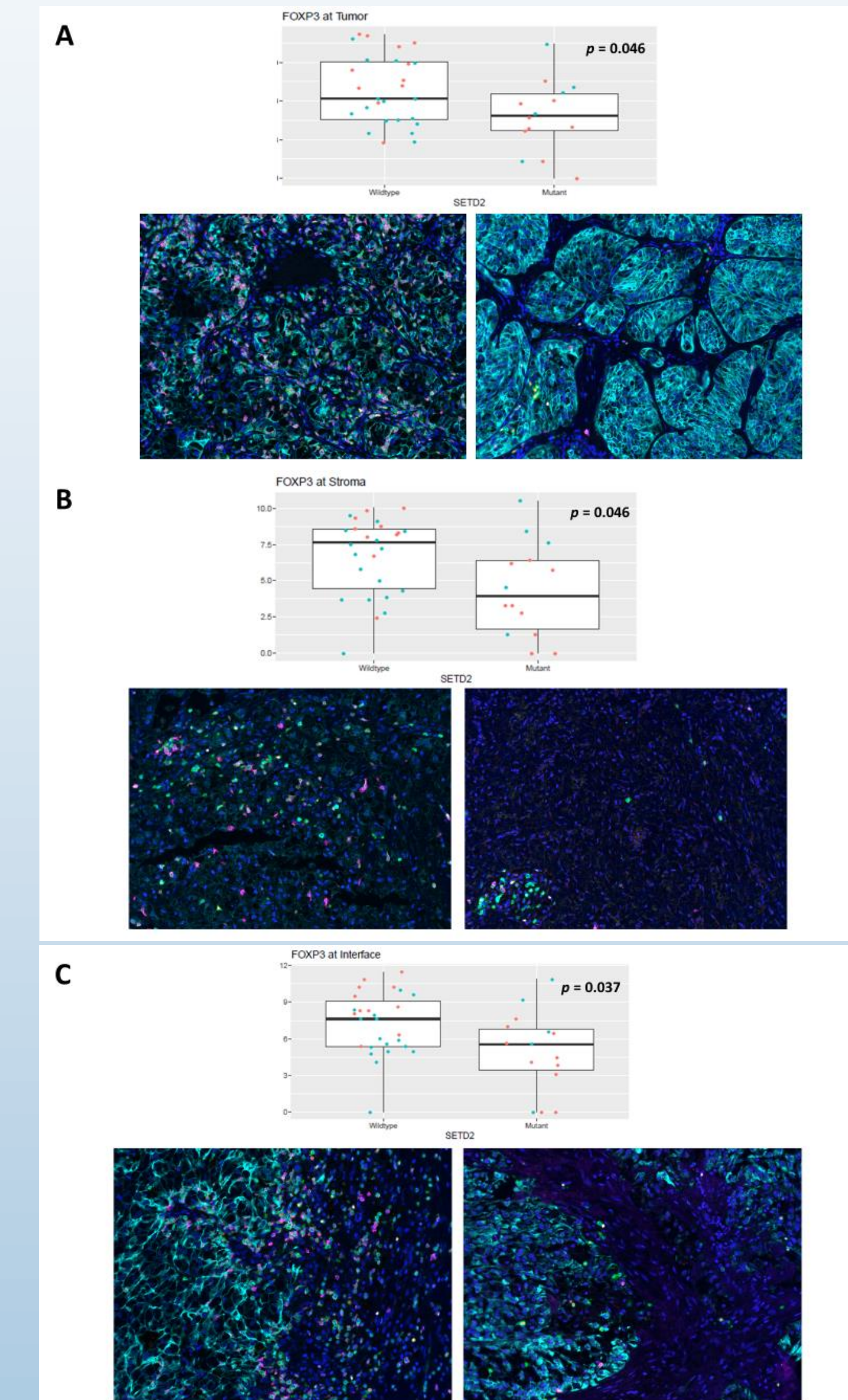


Figure 2. Box-plot diagrams for FOXP3+ cell density, stratified by SETD2 mutant status, with associated IF panels (FOXP3+ = pink, DAPI = dark blue, pan-cytokeratin = turquoise, CD3 = green, Tbet = yellow). A: Tumor-core, B: Stroma, C: Tumor-stroma interface.

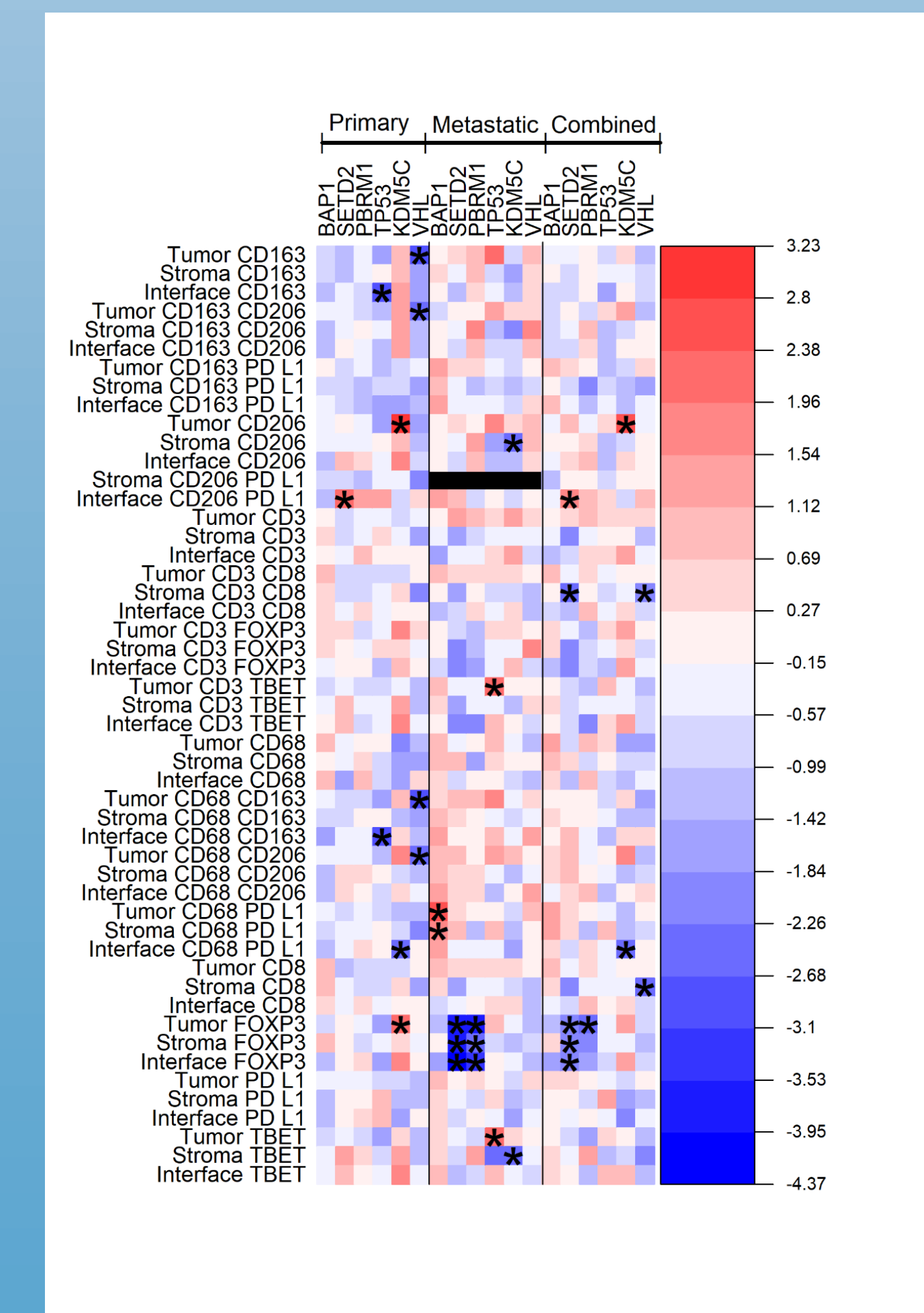


Figure 3. Heat-map diagram of immune cell density for all tumors, and primary and metastatic tumor subgroups. Asterisks represent p < 0.05. Stromal CD206+/PDL1+ unable to be assessed for metastatic tumors; too few cells identified.

Results

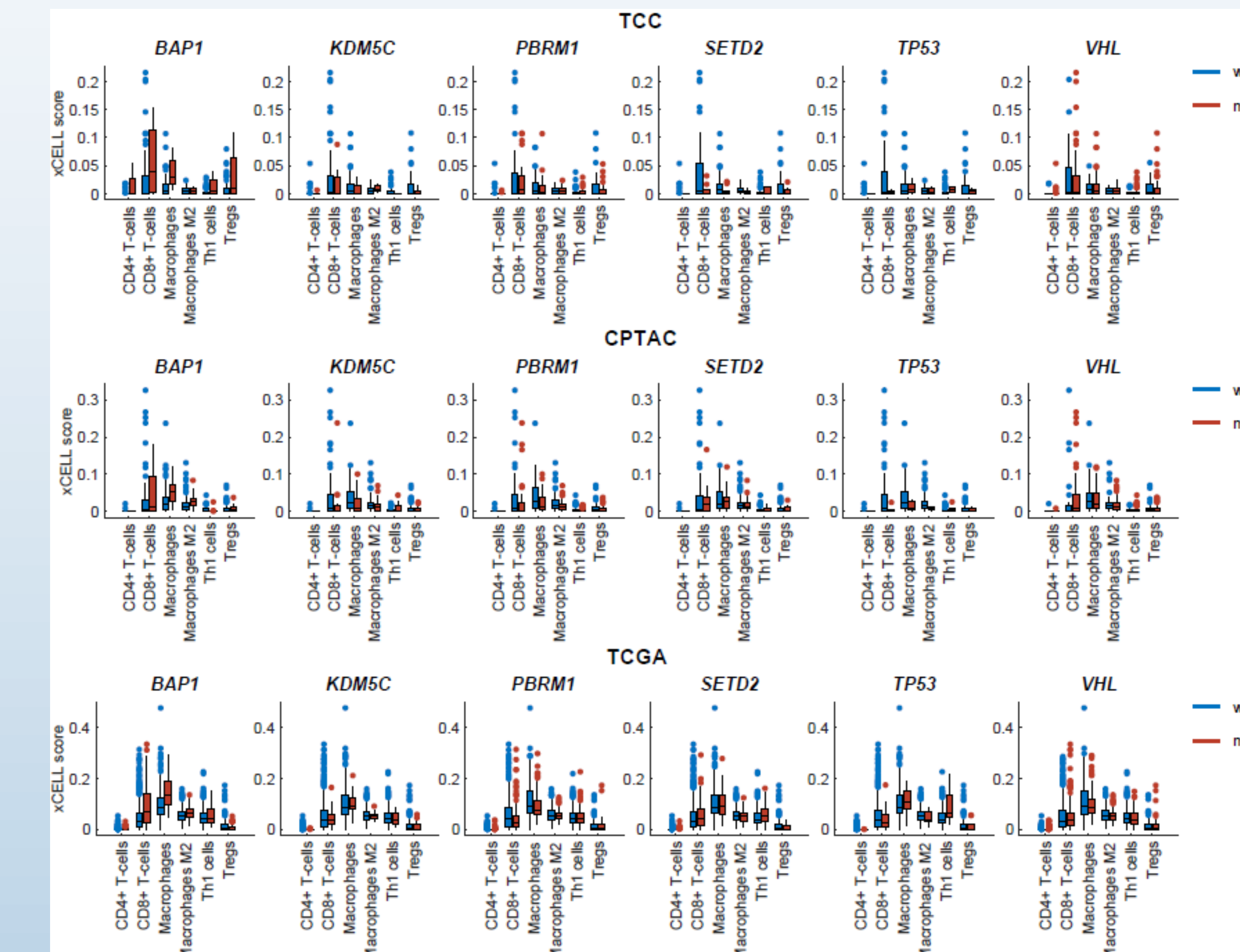


Figure 4. Box-plot diagrams for xCell enrichment scoring for selected cell types. RNA-seq data obtained from TCC, CPTAC, and TCGA cohorts.

Gene	# Immune Infiltration			xCell Enrichment Score		
	Tumor	Stroma	Interface	TCGA	CPTAC	TCC
BAP1						
CD8						
Tbet						
FOXP3						
CD68						
CD163/206						
PBRM1						
CD8						
Tbet						
FOXP3						
CD68						
CD163/206						
TP53						
CD8						
Tbet						
FOXP3						
CD68						
CD163/206						
VHL						
CD8						
Tbet						
FOXP3						
CD68						
CD163/206						

Figure 5. Tables comparing statistically significant findings from the IF-derived immune infiltrate analysis and xCell enrichment scoring, for all tumor samples. Green panels represent increased infiltration or xCell score for mutants, and red represents decreased infiltration or xCell score for mutants.

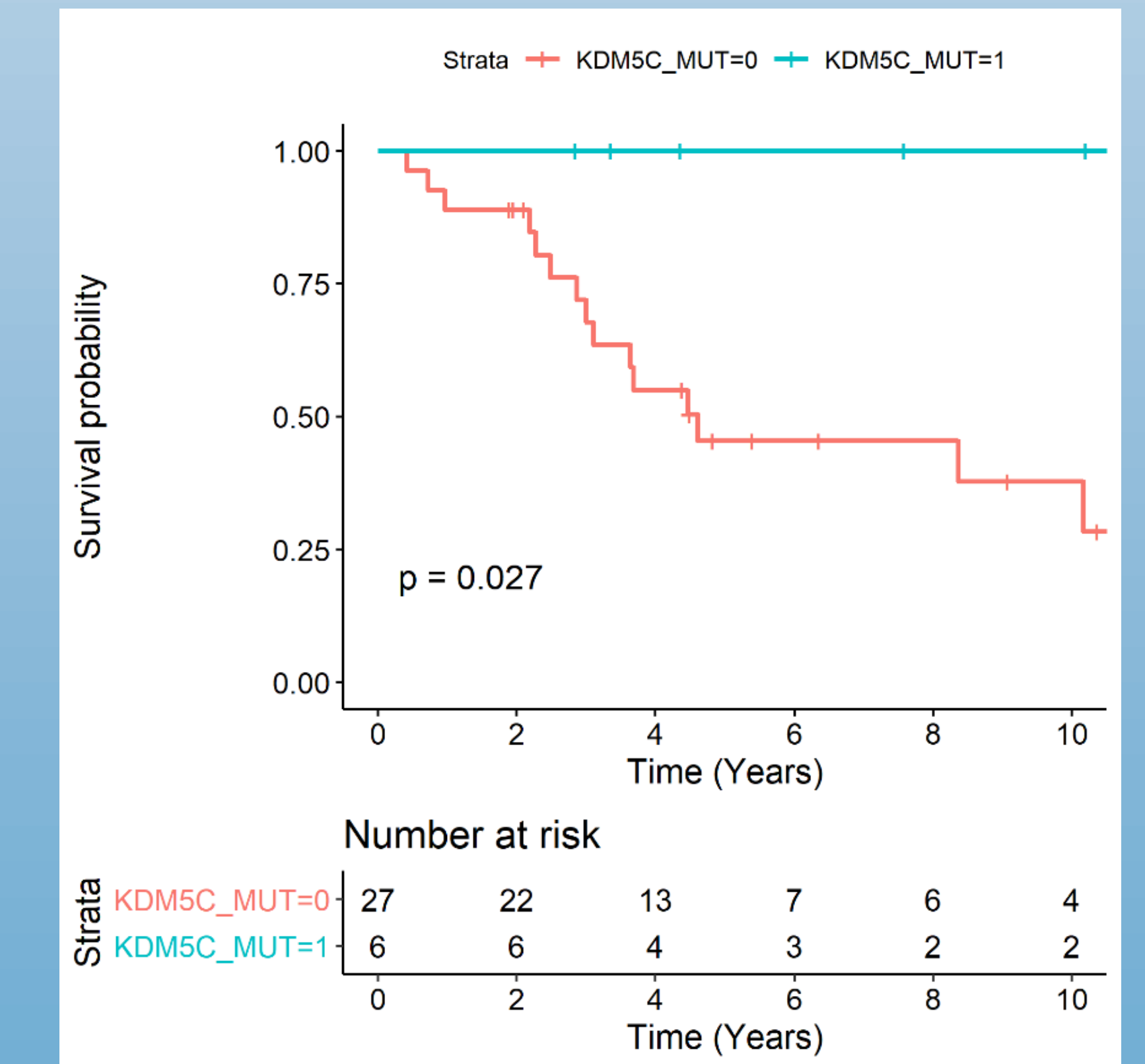
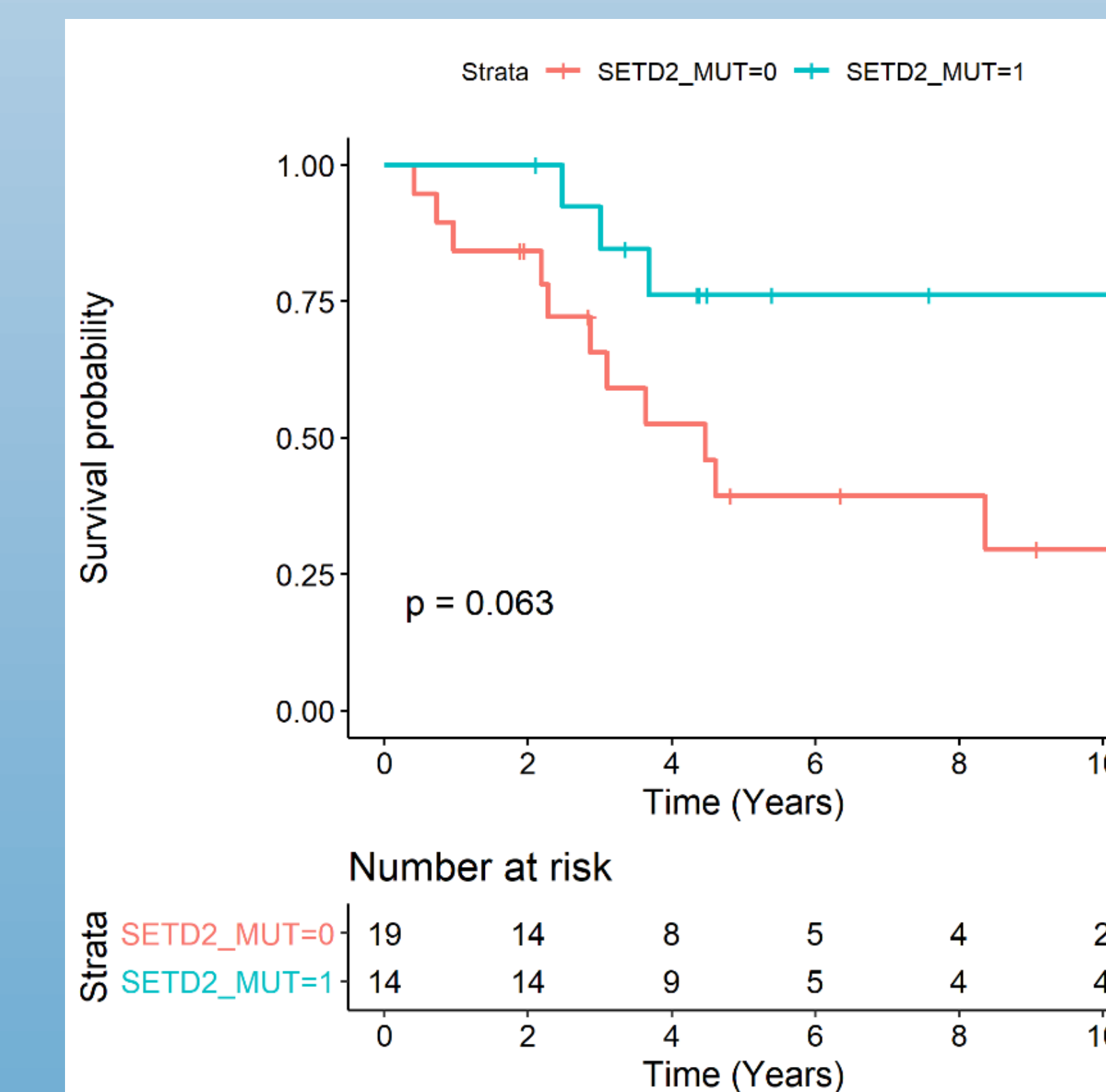


Figure 6. Kaplan-Meier survival analysis for OS in patients with (A) SETD2 and (B) KDM5C mutations.

Conclusion

This study provides evidence that common somatic mutations in ccRCC, such as SETD2, PBRM1, and KDM5C, may be associated with distinct immune infiltration patterns within the TIME. These novel associations have the potential to inform precision research and immunotherapeutic treatment strategies.